

Document downloaded from:

<http://hdl.handle.net/10251/80678>

This paper must be cited as:

Navarro Tarín, S.; Lerma García, JL. (2016). Accuracy analysis of a mobile mapping system for close range photogrammetric projects. *Measurement*. 93:148-156.
doi:10.1016/j.measurement.2016.07.030.



The final publication is available at

<http://dx.doi.org/10.1016/j.measurement.2016.07.030>

Copyright Elsevier

Additional Information

Accuracy analysis of a mobile mapping system for close range photogrammetric projects

Santiago Navarro, José Luis Lerma (jllerma@cgf.upv.es)

Photogrammetry & Laser Scanning Research Group (GIFLE), Department of Cartographic Engineering, Geodesy and Photogrammetry, Universitat Politècnica de València

Abstract

Image-based mapping solutions require accurate exterior orientation parameters independently of the cameras used for a survey. This paper analyses the inclusion of up to two stereo-based geometric constraints in the form of baseline distance and convergence angle between camera axes to boost the integrated sensor orientation performance on outdoor close-range projects. A terrestrial low-cost mobile mapping GNSS/IMU multi-camera system is used to test the performance of the stereo-based geometric constraint on a weak geometric network in a stop-and-go survey. The influence of the number of control points (CPs) is analysed to confirm the performance and usability of the geometric constraints in real live terrestrial projects where far from ideal setups can exist across the survey. Improvements in image residuals up to 9 times and deviation errors better than 1 cm are expected when at least three CPs are incorporated into the adjustment.

Keywords: georeferencing, integrated sensor orientation (ISO), close range photogrammetry, mobile mapping, stereo-based constraints

1. Introduction

The integration of global navigation satellite systems (GNSS) such as GPS, Glonass, Galileo and Compass and inertial measurement units (IMU) with data acquisition sensors of different nature both optic (high resolution cameras, video-cameras and multispectral sensors) and non-optic (radar, laser scanner) are becoming essential tools especially in multi-sensor mobile mapping systems for navigation, georeferencing, surveying, updating databases and data flow optimization [1]. The concept of using GNSS/IMU for direct georeferencing of aerial images emerged in the 1980's and early 1990's [2]. Differential GNSS combined with high accuracy inertial systems were successfully used to determine the full exterior orientation for photogrammetry. Accurate direct georeferencing alleviated the need of ground control in object space and has long been optimised for mobile mapping systems that integrate multiple image-based and navigation sensors. At present direct georeferencing is used to determine the orientation of many sensors such as digital cameras, video-cameras, LIDAR and SAR. In many cases it is the only way to georeference the sensor.

Comprehensive scientific references can be found in the literature about the performance of airborne direct georeferencing [3,4]. Some of the undertaken studies estimate the accuracy and reliability of direct georeferencing in an operational photogrammetric environment considering varying baseline distances to the master GNSS station and variable image overlap [5]. [6,7] report on the missing reliability of the direct determination of sensor orientation. In fact, the model setup often leads to unacceptable y parallaxes. A combined bundle block adjustment (also known as ISO or mixed georeferencing) is the recommended way to solve direct georeferencing issues. [4] confirms that ISO represents the security net for direct georeferencing and is inevitable for the system calibration. [8] suggest that including a minimum of one tie point per model is recommended to reduce y parallax within the ISO approach.

Likewise airborne mapping systems, land-based mobile mapping systems with multi-sensor integrated technology rapidly developed in the market. An exhaustive review of different mobile mapping systems can be found in [9–12]; the two latter ones including also mobile laser scanning systems. The trend is to include cheaper, smaller and less stable inertial sensors based on Micro Electronic Mechanical Systems (MEMS) as reported in [13], for instance in low-cost close-range photogrammetry [14–16] and smartphone-based technology [17,18]. Other low-cost mobile mapping systems do not even incorporate IMU but rely the orientation of the images either on a bundle block adjustment solution [10] or on stereovision [19]. Another low-cost mapping system incorporates a digital compass and a 3D city model [20]. Robotics is another field where simultaneous location and mapping (SLAM) systems are highly developed for autonomous vehicle guidance [21]. Robust localisation of vehicles is required as well as improved navigation systems. Low-cost stereo cameras and low-cost GPS are the primary sensors. When the navigation GPS signal is not available, the system relies on visual information through stereovision which only provides local relative information. Nevertheless, the recovery of accurate data from stereo as a primary sensor requires a careful precise calibration of the exterior orientation parameters [19]. Highly automated and highly accurate close-range photogrammetric solutions are required for instance in industry [22] and medicine [23]. For outdoor applications, less demanding (accurate) photogrammetric solutions are requested for recording. Nevertheless, accurate georeferencing (centimetre level) is required to fit geospatial information on different cartographic databases, GIS and BIM namely at national and regional scales, notwithstanding local large-scale global market require absolute coordinates.

The use of geometric constraints can be introduced for better spatial orientation of image-based multi-sensor systems. Constraints in form of observations can be included into the mathematical model of bundle adjustment to enforce certain requirements in object space [24]. The inclusion of relative constraints on the image-based sensors, fixed/free points, pre-set angular values, vectorial and distance equalities and parallelism/orthogonality/planarity/symmetry/alignment conditions can be found [25,26]. Extending the mathematical model with constraints reduce both the variance of the estimated parameters and the correlations between parameters, and increase the redundancy of the model [27]. As expressed in [28], in the least-squares adjustment the relative orientation parameters between stereo-pairs

at every exposure can be realised by adding equations/observations [29–34], or integrated directly into the collinearity equations [35]. In the latter paper, a bi-camera system coupling two multispectral cameras is used. However, the solution of the exterior orientation parameters of the low resolution camera is based on the transfer of the exterior orientation of the high resolution camera after constraining the relative orientation of the bi-camera system.

Besides, stereo-based geometric constraints provide spatial information to the adjustment and can be used to orientate or scale the model without the need to measure distances from the captured object. This property is useful for automatic orientation processes based on structure from motion [36]. However, its use is not presently widespread for georeferencing low-cost land mobile systems. The use of constraints in GNSS/INS systems has been used to improve not only the camera orientation [27] but also the boresight calibration for aerial multi-head camera systems [31,37]. Considering that the multi-head system is tightly affixed to the camera platform, the geometric calibration can be considered constant while acquiring data. In case of instabilities, the weights of the observations can be adjusted to consider small movements of the camera heads [31]. In both studies, the results show better accuracy and better precision than the bundle adjustment without constraints. [32] included baseline distance constraints in a general bundle adjustment solution for the geometric calibration of a mobile mapping system that integrates multispectral sensors of different nature, with outstanding improvements in the estimation of both the interior and the exterior orientation parameters especially of the low-resolution camera. [38] reported on a simultaneous geometric calibration of multi-cameras using relative orientation constraints, advising that higher weights could lead to inaccurate results. [39] dealt not only the geometric calibration with relative orientation stability constraints of a multi-head arrangement but also the registration/fusion effects when generating virtual images. This latter paper reviewed in detail the topic of stereo camera system calibration considering the use of relative orientation constraints, and reported different formulation that might be used as relative constraints in the bundle adjustment. In our implementation, the way the relative orientation constraints are included into the general bundle block adjustment solution is slightly different from previous ones [31,38,39]: it follows a general least squares adjustment, it is compact (i.e. only four additional equations are included in the overall adjustment at different time instants), the global constraints are based on both convergence angle between camera axes and baseline distance, and the behaviour of the exterior orientation parameters can be easily weighted through the additional equations.

This paper makes use of a low-cost GNSS/IMU multi-camera system to undertake ISO in stop-and-go mode. It means that the system acquires the data in static mode for fixed periods and processes off-line navigation and final photogrammetric orientation for each station. Relative stereo-based geometric constraints (convergence angle and baseline distance) between optical sensors are included in the ISO to test their influences on a weak geometric network with varying number of control points (CPs). By weak geometry it is understood that just a few and badly distributed tie points between images in stereo-pair setup can be found due to both lack of image texture (e.g. ground and sky presence, homogeneous facing on

buildings, etc.) and different spatial resolution of the integrated image-based sensors (herein visible digital cameras). Moreover, when using imaging sensors of different wavelength response. Furthermore, the influence of control points in the final object space estimates is analysed. The study presented herein demonstrates the benefit of including both stereo-based geometric constraints on mobile mapping systems that combine diverse imaging sensors, as they help the orientation of the image-based sensors based on the number of available CPs.

2. Description of the mobile multi-camera system

The mobile GNSS/IMU multi-camera system integrates a primary (vertical) cylindrical body with the IMU inside on a rotating horizontal secondary cylinder where the optical sensors are attached. On the top of the main body lies the GNSS antenna, forming a uncoupled GNSS/IMU. The benefit of this type of integration on the multi-camera system is its flexible and economic configuration, easy and quick to assemble. Furthermore, it provides some tolerance to failing on the subsystem components.

At the ends of the secondary cylinder are located the supports where multiple imaging sensors can be placed. The cameras can be turned around the secondary axis of the system and attached enabling both stereoscopic and convergent shots. The system allows through the secondary cylinder a rotation around the x-axis that eases changing the vertical direction of the camera's point of view. The IMU is centred in the intersection of the primary and secondary axis. The primary axis of the cylindrical body has to be perfectly levelled to guarantee that the GNSS antenna is on the vertical of the IMU sensor.

The design takes into account that the GNSS antenna has to be always vertical, in order to have a good horizontal coverage for signal reception avoiding any obstruction that may cause losses of signals. In the top centre, there is a chance to add a vertical arm extension to avoid blocking the reception of the GNSS signal (Fig. 1). Information relative to the indoor and outdoor calibration of the whole multi-sensor system can be found in [16].

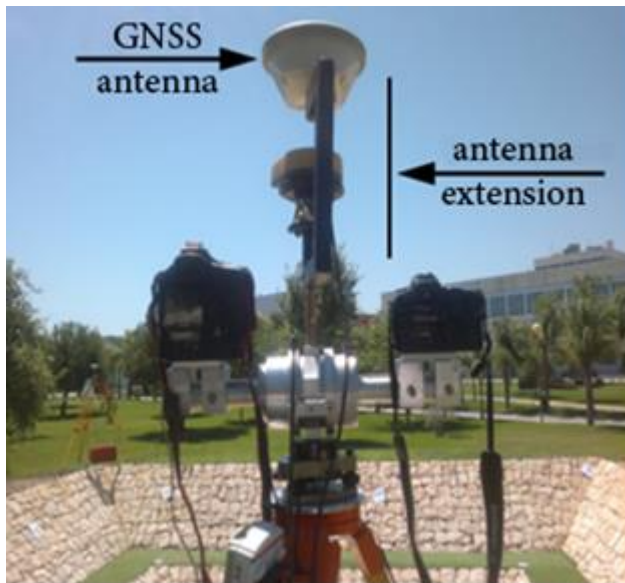


Fig. 1. Mobile stop-and-go GNSS/IMU multi-camera system on a surveying tripod.

This particular mobile multi-sensor system was developed in our university. It is a variant (second evolution) of our first developed rigid body GNSS/IMU multi-camera system [32]. The main advantage of this solution is that it can be used to avoid losses of GNSS signals while shooting non-horizontal structures such as bridges, buildings, drains, mountainsides, etc.

3. Integrated Sensor Orientation Methodological Approach

The external orientation parameters obtained by the GNSS/IMU direct georeferencing will be used to determine the ISO of the mobile GNSS/INS multi-camera system by means of a least-squares adjustment, measuring homologous image coordinates across the set of images. The same image data will be used to get a first calibration of the interior orientation parameters and exterior orientation parameters of the mobile multi-camera system. Fig. 2 displays the integration sensor orientation workflow carried out with the mobile mapping system; the main geometric results obtained in each step are also presented. First, the cameras that will be coupled to the mobile multi-camera system are calibrated to achieve the preliminary calibrated interior orientation parameters. Later follows the navigation and data acquisition on-site full of CPs and check points (ChPs). In each station, the mobile stop-and-go multi-camera system is stopped for 15 s to acquire both navigation datasets (GNSS/IMU) and imagery. Further information about this point is presented later in the Experiments and Results Section. With the second data set acquired in the field, a new field calibration is undertaken to estimate better the interior orientation parameters of the cameras at the working distance. Later the mobile GNSS/INS multi-camera system is calibrated, giving as a result the vectors a

(IMU-CAM), b (IMU-GNSS), translation and drift as a function of time, and misalignment matrix R_{IMU}^{CAMm} . The general least squares adjustment is used to determine the best solution [40]. As the calibrated interior orientation parameters were optimally determined in the previous step, they were not included herein: the interior orientation parameters were constraint. Nevertheless, it is up to the user (specialist) due to the flexibility of the mathematical model. A complete description of the geometric calibration of the mobile mapping system for direct georeferencing can be found in [16]. This paper concentrates on the latter step presented in Fig. 2, georeferencing analysis and performance of the ISO with the inclusion of stereo-based geometric constraints.

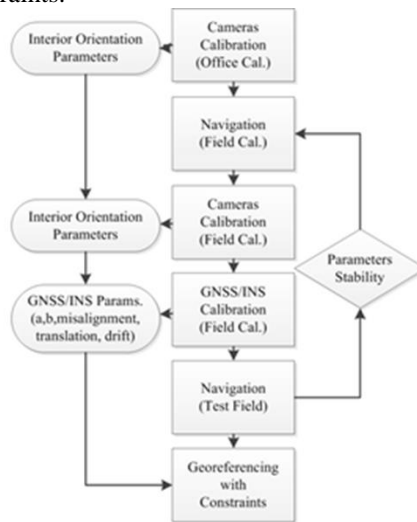


Fig. 2. Workflow for the integrated sensor orientation (ISO) with geometric constraints.

The in-house photogrammetric software FOTOGIFLE is used to process the data coming from the multiple sensors on the mobile multi-camera system to calibrate, orient and eventually generate photorealistic 3D models.

4. Georeferencing with Geometric Constraints

Given the characteristics of the photogrammetric GNSS/INS system and assuming that the relative positions between the sensors are stable, various types of geometric constraints can be applied. In particular, two stereo-based constraints are considered: first, baseline distance constraint; second, convergence angle constraint; and third, the simultaneous incorporation of both the baseline distance constraint and the convergence angle constraint. It is mandatory to weight the different geometric conditions once the constraints are introduced into the integrated bundle adjustment. The geometric conditions enforce the least squares solution to satisfy the constraints added to the system.

The baseline (base) distance constraint (Fig. 3) fixes the distance between perspective centres. Thus, the adjustment converges to a solution where the

perspective centres of the cameras minimize the residuals in all camera stations where the cameras keep the same distance [29,32].

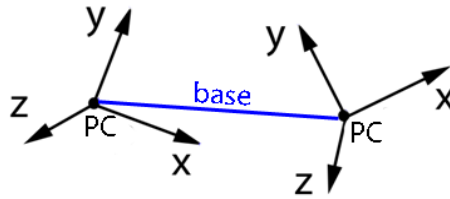


Fig. 3. Baseline distance constraint.

$$Base_{ij} = \sqrt{(X_i - X_j)^2 + (Y_i - Y_j)^2 + (Z_i - Z_j)^2} \quad (1)$$

Eq. (1) has to be linearised in order to be included in a general least squares adjustment [32]. There are up to six unknowns, one for each coordinate of the perspective centre of the two cameras (subindex i denotes principal camera and subindex j secondary camera). The weight used for the baseline distance constraint is proportional to the precision error in the observed baseline distance.

The second stereo-based constraint considered is the convergence angle between camera axes due to the fact that both cameras affixed to the mobile mapping system maintain the same orientation between them for a survey. This condition enforces that the convergences of the axes of the cameras are the same for all the stations (Fig. 4).

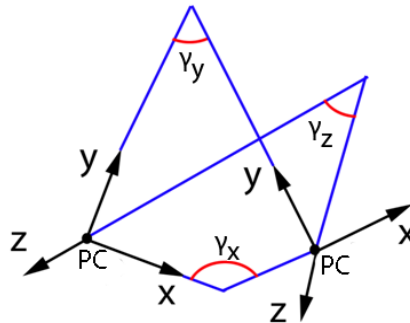


Fig. 4. Convergence angle between camera axes from two perspective centres (PC).

From Eq. (2) the convergence angle γ for each axis is obtained:

$$\begin{aligned} \gamma_x &= \cos^{-1}(\mathbf{R}\mathbf{x}_1 \cdot \mathbf{R}\mathbf{x}_2) \\ \gamma_y &= \cos^{-1}(\mathbf{R}\mathbf{y}_1 \cdot \mathbf{R}\mathbf{y}_2) \\ \gamma_z &= \cos^{-1}(\mathbf{R}\mathbf{z}_1 \cdot \mathbf{R}\mathbf{z}_2) \end{aligned} \quad (2)$$

Being \mathbf{R} the corresponding camera rotation matrix for the first, 1, and the second, 2, camera, respectively. The linearisation of Eq. (2) yields three equations that relate the convergence of the axes with the angles of the camera rotation matrices as unknowns. During the integrated bundle adjustment, the constraints force the orientation parameters of the cameras to meet the geometry based on the weighting.

5. Experiments and Results

This section presents the experiments undertaken with the mobile GNSS/INS multi-camera system on site in the calibration field. In particular, the sensors mounted on the GNSS/INS multi-camera system as well as the ISO with stereo-based geometric constraints will be presented under conditions of weak geometry between imaging sensors on each station.

5.1 Setup

The calibration field used to test the performance of the ISO with geometric constraints is displayed in Fig. 5. It follows an inverted pyramidal structure measuring 9 m x 9 m x 2.67 m. The calibration area is full of control, whence 4 are CPs and 39 ChPs; the accuracy of the point coordinates is better than 5 mm. A total of 26 stations surrounding the site were taken in stop-and-go mode (acquiring GPS and IMU data for 30 s on each stop) from the top, following a closed traverse with parallel shots on each side and convergent shots at the corners. An over redundant integrated bundle block adjustment (with large number of degrees of freedom) followed to achieve a precise estimation of the parameters.

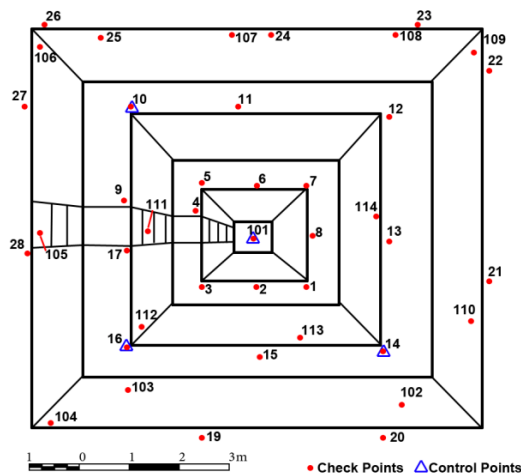


Fig. 5. Distribution of CPs and ChPs on the geometric calibration field.

The sensors mounted on the GNSS/IMU multi-camera system were one GPS RTK Trimble 5700 double frequency with 24 channels and long battery life. WAAS and EGNOS capabilities allow users to perform real-time differential surveys to GIS applications without a base station. The IMU used was a low-cost MEMS IMU Mtx from Xsens Technologies. This IMU sensor yields a static accuracy for roll and pitch $< 0.5^\circ$ and heading $< 1^\circ$; and a gyro bias stability of $20^\circ/\text{h}$.

The photogrammetric image-based sensors used for the tests were two single lens reflex (SLR) digital cameras with different features: Canon EOS 1D Mark III (full frame sensor, 21.9 Mpixel) with Canon lens EF 24 mm F2.8 and Canon EOS D60 (APS-C sensor, 6.3 Mpixel) with Sigma lens 15-30 mm F3.5-4.5 EX DG; the former was used as primary camera and the latter as secondary. The low-resolution of the secondary camera was considered to be able to extrapolate the benefits of constraining true multi-camera systems independently of the imaging sensor used (ultraviolet, visible, near infrared, thermal, terahertz...). In fact, non-visible imaging sensors are usually low-resolution.

To study the behaviour of the geometric constraints under non-ideal setup (imagery with large portion of sky, lack of homologous features between primary and secondary cameras, adverse background and foreground), weak tie point matching between images was undertaken (Fig. 6): 3 or 4 tie points with randomized distribution (from a hierarchical automatic feature-based matching and area-based matching scheme as reported in [41]) were used to tie the secondary camera images with the principal camera images at the exposure time (these point will be denoted as tpA); CPs only appear on the principal camera images. Tie points on the principal camera images (tpB) are properly allocated and distinct of tpA; secondary camera images are not linked together except by ChPs (which are not taken into consideration in the bundle block adjustment).

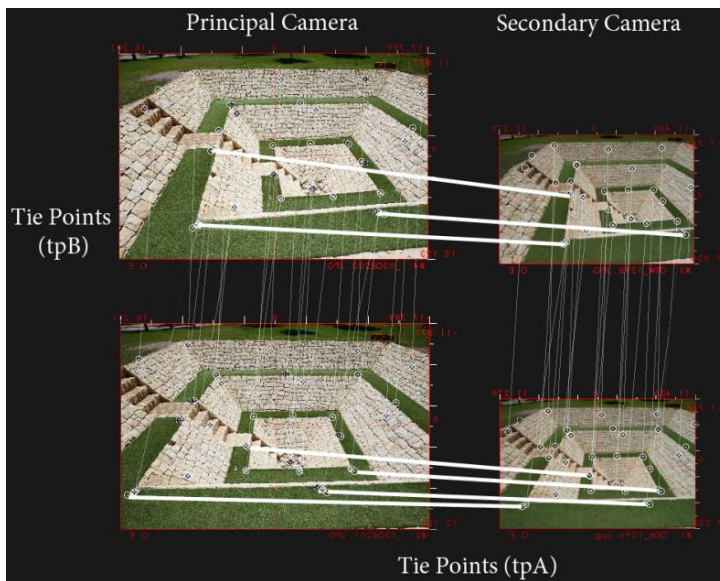


Fig. 6. Tie point matches among different imagery: principal camera (tpB); principal and secondary camera (tpA).

5.2 Direct Georeferencing vs Integrated Sensor Orientation

The performance of the Direct Georeferencing (DG) was analysed in the calibration after the mobile GNSS/IMU multi-camera system was successfully calibrated. Only

the ChPs were used to determine the deviations in object space. The differences between the 37 surveyed ChPs and calculated photogrammetric points following DG forward intersection yielded an average value of 0.14 m and a maximum deviation value of 0.31 m (Fig. 7). Besides, after ISO with the georeferenced data, the weak geometrical disposition of the CPs and tie points on the principal and secondary camera yielded worse results than DG: average deviation error of 0.29 m and maximum deviation error of 0.54 m; the unexpected better DG result is namely due to the weak geometric network created for the close range adjustment and poorly distributed tie points. In this kind of scenario, the improvement of the ISO after introducing the stereo-based constraints is tested in the next section. Besides, the expected a priori accuracy for a normal case survey considering a maximum distance of 10 m, a principal distance of 0.024 m and a baseline distance of 0.40 m is better than 0.04 m (1 sigma). Next section analyses the influence of the CPs and the baseline distance constraints in the final solution (that should be better than the estimated a priori accuracy).

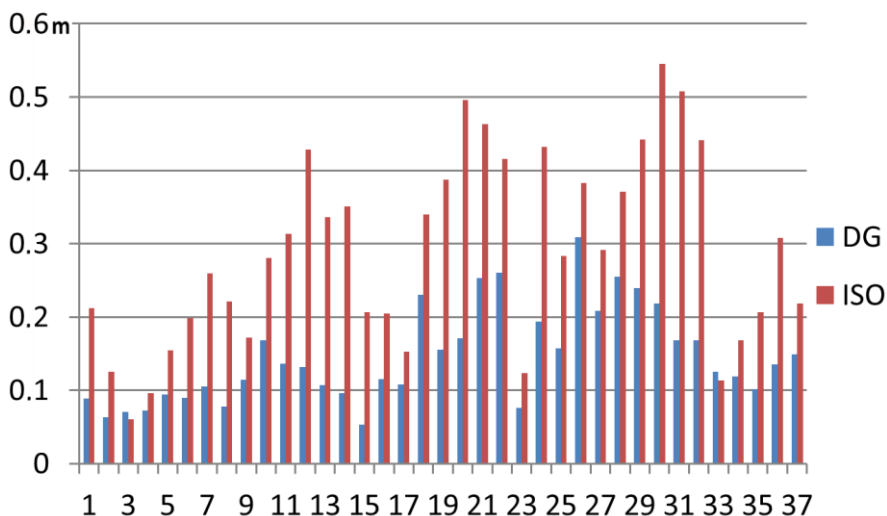


Fig. 7. Deviation errors (in m) after DG and ISO on the 39 ChPs.

The analysis of the residuals after ISO on the imagery affects differently each camera. The principal camera has good tie point matches between the images, and the maximum deviation after reprojection reaches 1.5 pixels. However, the secondary images reach up to 52.67 pixels and an average deviation error of 7 pixels. These bad results in the secondary camera are attributed to the lack of CPs in the bundle block adjustment and the weak tie point matches. In any case, the improvement of the weak network geometry will be empirically demonstrated next.

5.3 Integrated Sensor Orientation with stereo-based geometric constraints and influence of the number of control points

The used mobile GNSS/IMU multi-camera system had two cameras of different spatial resolution. Therefore, it was considered best to calibrate independently both of them. Once calibrated a conventional bundle block adjustment with fixed CPs was undertaken to determine the relative orientation between the cameras from which both stereo-based geometric constraints are determined (Table 1) and used for the subsequent ISOs. As the multi-camera system is very stable, the constraints keep constant throughout the survey; it took maximum a couple of hours. The stability is controlled by the constraint weights, which can be modified in each general least squares adjustment [32,40]. Nevertheless, over-constraining or under-constraining an adjustment is reflected straight-ahead on the least squares results.

Table 1. Estimated constraints and related standard deviations regarding convergence angle (γ) and baseline distance (*Base*) used for ISO with constraints.

γ_x	γ_y	γ_z	$\sigma\gamma_x$	$\sigma\gamma_y$	$\sigma\gamma_z$	<i>Base</i>	σ_{Base}
1.1698°	1.1813°	1.6259°	0.0022°	0.0022°	0.0022°	0.401m	0.0001m

Several integrated bundle block adjustments introducing different geometric constraints (none, baseline distance, convergence angle, and baseline distance plus convergence angle) and different number of CPs were undertaken in order to test the performance of the stop-and-go mobile mapping solution. The CPs were introduced gradually into the ISO starting from 0 up to 4 (CP numbers 101, 10, 16 and 14 in Fig. 5). The weights of each observation, exterior orientation parameters and constraints (Table I) were obtained from the previous bundle block adjustment used to calibrated each camera. Fig. 8 shows the error deviations at the check points according to the number of CPs introduced in the adjustment and the type of constrained applied. ISO without control points (0 CP) yielded an average error of 0.29 m, 0.27-0.28 m introducing one single constraint and 0.21 m with both constraints, which means an improvement of 28% compared to not using any stereo-based geometric constraint or just 25% using a single constraint on the multi-camera system. The difference of using 0 CP or just 1 CP is negligible. Only with 2 CP the deviation errors are stabilized around 0.26 m. With three CPs or more, there was a dramatic improvement in the results, mean differences below 0.03 m without stereo-based geometric constraints, improving to 0.02 m with the baseline distance constraint, 1 cm with the convergence angle constraint and down to 0.005 m when the two stereo-based constraints are included in the bundle adjustment.

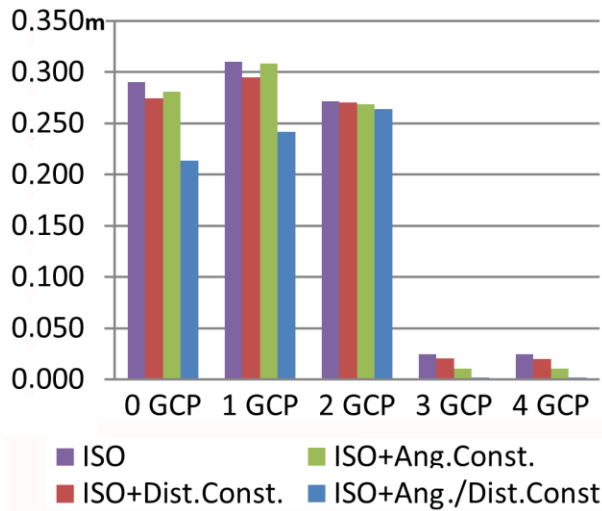


Fig. 8. Average ISO deviation errors in object space at the ChPs depending on the number of CPs.

This increased accuracy in determining the imaging sensor orientation is reflected not only in object space but also in a substantial reduction of the image residuals (Fig. 9). Without CPs and two constraints an average residual of 1.6 pixels is achieved compared to 3.7 pixels with standard integrated bundle adjustment. When 2 or more CPs were included, the inclusion of the distance constraint yielded smaller image residuals (approx. 3.2 pixels instead of 4.6 pixels), even better were achieved with the convergence angle constraint (approx. 1.9 pixels) was included, to achieve the best image residuals down to 0.3 pixels when the two set of stereo-based constraints were integrated into the ISO. It can also be observed that the application of both geometric constraints, baseline distance and angle convergence angle between sensors, provides always better adjustment estimations than constraining the adjustments with just one single constraint and significantly better estimations than in conventional ISO.

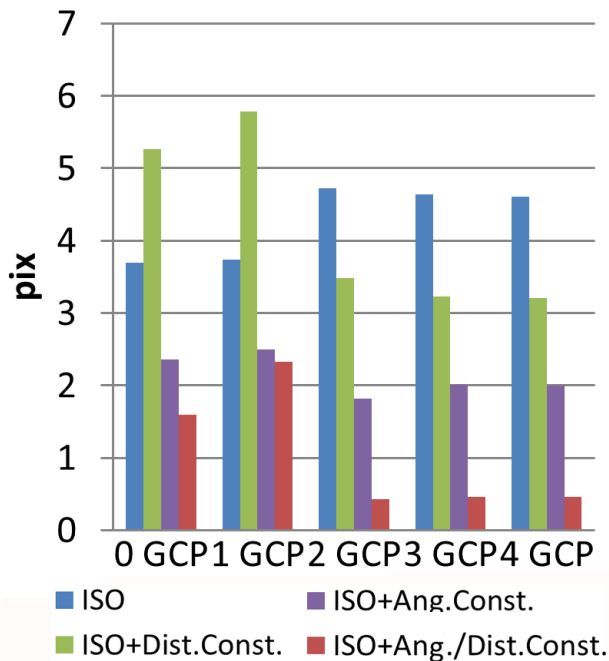


Fig. 9. Average ISO residuals according to the number of CPs.

The effect of the two stereo-based geometric constraints in the precision of the estimates after ISO was also determined (Fig. 10). The error in the determination of the Euler rotation parameters (Omega, Phi and Kappa) without constraints was between $0.01^{\circ} - 0.06^{\circ}$ (except for photo 24 with a value of 0.25°). With two stereo-based constraints included in the ISO the estimates improved most of the times 10x; worth noticing was the improvement up to 100x for station positions with weak geometry.

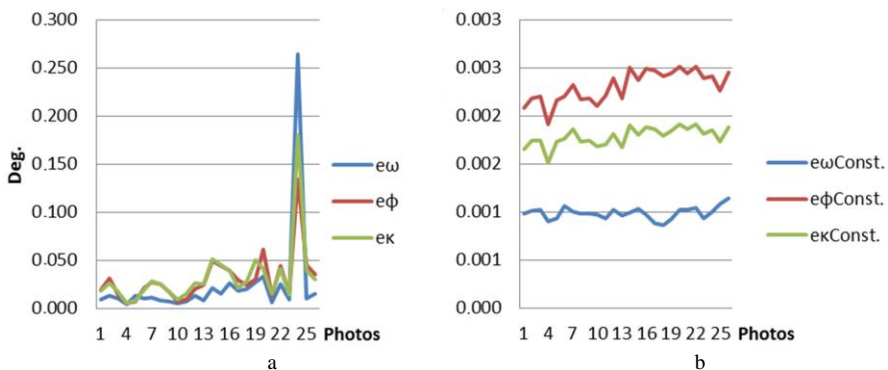


Fig. 10. Standard deviation of the three angles after ISO: a) standard solution without constraints; b) with the two stereo-based constraints.

Similarly to the determination of the rotation angles of the optical sensors, the inclusion of stereo-based geometric constraints between cameras substantially improved the determination of the projection centres coordinates, obtaining a maximum error of 0.02 m for the ISO without any constraint and below 0.003 m with the inclusion of both constraints (Fig. 11).

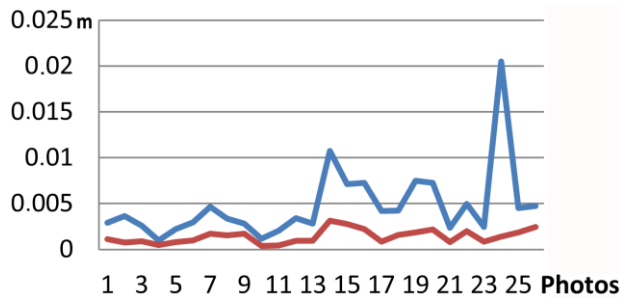


Fig. 11. Overall standard deviation of the projection centre. Blue: ISO; Red: ISO + Const.

The ISO approach with the inclusion of the two stereo-based constraints benefited the photogrammetric performance not only for the orientation stage but also for dense matching. A robust solution will always yield better image residuals and therefore closer corresponding features to the epipolar constraint. Fig. 12 displays the 26 station positions with the stereo-based setup surrounding the calibration field. The dense point cloud matching followed the strategy presented in [41] to achieve subpixel accuracy in the image space: first feature-based matching with either SURF or SIFT at the highest pyramidal level, second normalized cross correlation and finally least squares matching (LSM) at the lowest pyramidal level in the UTM system.



Fig. 12. 3D point cloud and spatial configuration of the navigation. View from the top.

6. Discussion

The precision obtained in DG depends basically on the precision of the acquired GNSS and IMU data plus the system calibration (including offsets, misalignments and camera calibration). The higher precision of the estimates the lesser need of CPs. The approach presented herein considered GPS RTK and low-cost IMU MEMS in stop-and-go mode to determine DG. Therefore, the presented approach is not a dynamic solution but user's mobile, flexible and affordable multi-sensor solution worth considering for many geoscience, engineering and cultural heritage applications outdoor.

According to the results obtained for a maximum camera-object distance of approximately 10 m, an average 0.14 m deviation error in object space (Fig. 7) when computing object coordinates after DG and forward intersection can be enough accuracy for non-demanding close range projects. The deterioration of the ISO without constraints when the CPs are not properly distributed across the surveying area is also manifested. The error budget derived from the low-cost raw IMU values is manifest; the errors in the GNSS positioning, boresight misalignment and relative orientation of the cameras are very low whether the multi-camera system is properly calibrated.

Both stereo-based geometric constraints improved strongly the solution of the secondary camera regarding both the precision of exterior orientation parameters and the computation of points in object space. The combination of the two stereo-based geometric constraints, base length (base) constraint and convergence angle versus the use of one single constraint is outstanding: without CPs the results improve up to 25%; with 3 or more CPs, up to 36%.

Both cameras might have been simultaneously calibrated in the bundle block adjustment using geometric constraints whether the relative orientation between cameras mounted on the multi-camera system was already known [39]. The stereo-based geometric constraints reduce the need of CPs whenever incorporating imaging sensors of different resolutions (Fig. 8). For instance, just with 3CPs, the ISO without geometric constraints was in an average deviation error of 0.03 m approx. while the ISO solution with two stereo-based geometric constraints was 0.002 m. The solution of the ISO with both angular and distance constraints yielded better results than single separate constraints (Fig. 8), not only in object space but also in image space (Fig. 9). With 3 or more CPs, the improvement in the quality of the object coordinates was smaller than 2x when incorporating single constraints, and smaller than 10x when incorporating both stereo-based geometric constraints.

The importance of matching properly image features is worth mentioning. Fig. 7 displays the importance effect of weakening a correct configuration of tie points. Even including stereo-based geometric constraints, it was required to consider a minimum of 3 CPs to achieve deviation errors below 0.01 m. This result is slightly different to the one presented in [15] which confirmed that with a proper configuration, at a distance of 10 m from the object, it was possible to achieve 0.0059 m deviation errors with only 1 CP. Our research only confirms this latter statement when 3 or more CPs are included in the adjustment.

The exterior orientation solution obtained with the stereo-based geometric constraints in the integrated bundle adjustment yielded a more precise determination of the

orientation parameters of the imaging sensors (most of the times 10x but also 100x values can be obtained); the stability of the estimates was also evident (Figs. 10 and 11).

The ISO with stereo-based geometric constraints of distance and angle allows users to estimate better not only the exterior orientation parameters (Figs. 10 and 11) but also the 3D point clouds through dense image matching. Fig. 12 displays the output 3D coloured point cloud achieved with the multi-camera system, and the spatial distribution of the image frames along the perimeter of the object, pointing roughly to the centre.

This study demonstrates the benefit of including both stereo-based geometric constraints on mobile mapping systems that combine multiple imaging sensors, as they help the orientation of these sensors along with CPs. Both image-based sensors are interrelated through stereo-based constraints in a different way than [35] in which one sensor is used to transfer the exterior orientation to the second (low-resolution) sensor. Therefore, the orientation of the secondary sensor depends on the primary sensor, and there is no need to include additional free-handled camera stations to strengthen the block geometry.

From another perspective, the stereo-based orientation might be used to transfer back the orientation to the system whenever the navigation system fails [31]. The stereo-based constraints can also be used to introduce real information from the world into the object space, allowing the model to be oriented or scaled automatically, without any need of having direct contact with the object [36]. The maximum camera-object distance should be set before the survey in order to achieve accurate estimates of measurements in object space. The concept of this stereo-based geometric constraint goes beyond measurements from stereo-pairs but transferring of exterior orientation for matching and texturing with multispectral imagery. Furthermore, the approach presented herein can be extended to determine in a single step the calibration of the mounting parameters of the multi-camera system, as recommended by [33] for mobile mapping systems. Last but not least, the presented ISO approach can be easily extended to boost the Unmanned Aerial Vehicle (UAV) photogrammetric performance [42] when applying multiple imagery sensors, decreasing the requested number of GCPs to a minimum of three.

7. Conclusions

In this paper DG and ISO with GNSS RTK, low-cost MEMS IMU and stereo-based geometric constraints is tested on a mobile stop-and-go photogrammetric GNSS/IMU multi-camera system. The influence of including both the baseline distance constraint and the convergence angle constraint between projection centres is analysed to improve the exterior orientation of the cameras. The results confirm that the exterior orientation of the images is better estimated in object space whenever weak or poor geometries are found not only in object but also in image spaces. Whenever ISO is worsening, the inclusion of both stereo-based geometric constraints can be used to improve dramatically (up to 9x) the quality of the bundle adjustment in object space when 3 or more CPs are available; the simultaneous benefit in image space with both constraints is highly recommended with improvements up to 9x with 2 or more CPs.

Therefore, the inclusion of stereo-based geometric constraints is considered essential to achieve reliable orientations whenever there is either a lack of control information or a weak tie point configuration in the adjustment.

In view of the results it can be stated that the inclusion of both stereo-based geometric constraints (that relate the imaging sensors of the mobile GNSS/INS multi-camera system) in the integrated bundle adjustment can yield accurate georeferencing and reduce significantly the number of CPs; at least 3 CPs are recommended to satisfy most demanding surveys. The inclusion of both stereo-based geometric constraints is highly recommended whether low-resolution imaging systems such as thermal cameras, hyperspectral sensors, web cams, etc. are introduced in the mobile mapping system. Better georeferencing estimation of these devices is foreseen. Furthermore, it offers greater flexibility in photogrammetric block adjustment which reduces the computation time devoted to the accurate determination of the exterior orientation. Last but not least the results are more robust, stable and accurate particularly when using image sensors of different nature. Owing to the modularity of the design of the multi-sensor system where the cameras can be interchanged, moved, rotated or removed for transportation, each project or working session might need different set of stereo-based geometric constraints. A simple strategy to validate the calibration parameters of the whole system in each new session is being implemented and will be reported next.

Acknowledgements

The authors gratefully acknowledge the support from the Spanish Ministerio de Economía y Competitividad to the project HAR2014-59873-R. Contributions on direct georeferencing from professors Dr. Hernández-López, Dr. García-Asenjo and D. Garrigues are highly appreciated.

References

- [1] N. El-Sheimy, The development of VISAT-a mobile survey system for GIS applications, University of Calgary, 1996.
- [2] J. Hutton, M.M.R. Mostafa, 10 Years of Direct Georeferencing For Airborne Photogrammetry, in: *Photogramm. Week, Geo-Information-Systeme*, 2005: pp. 1–16.
- [3] M.M.R. Mostafa, K.-P. Schwarz, Digital image georeferencing from a multiple camera system by GPS/INS, *ISPRS J. Photogramm. Remote Sens.* 56 (2001) 1–12. doi:[http://dx.doi.org/10.1016/S0924-2716\(01\)00030-2](http://dx.doi.org/10.1016/S0924-2716(01)00030-2).
- [4] J. Skaloud, Reliability in direct georeferencing: an overview of the current approaches and possibilities, in: *EuroSDR Work. EuroCOW Calibration Orientat.*, Castelldefels, Spain, 2006: pp. 1–14.
- [5] M. Cramer, D. Stallmann, N. Haala, Direct georeferencing using GPS/inertial exterior orientations for photogrammetric applications, *Int. Arch. Photogramm. Remote Sens.* 33 (2000) 198–205.
- [6] K. Jacobsen, Potential and limitation of direct sensor orientation, *Int. Arch. Photogramm. Remote Sens.* 33 (2000) 429–435.

- [7] N. Yastikli, K. Jacobsen, Direct Sensor Orientation for Large Scale Mapping-Potential, Problems, Solutions, *Photogramm. Rec.* 20 (2005) 274–284. doi:10.1111/j.1477-9730.2005.00318.x.
- [8] K. Khoshelham, Role of tie points in integrated sensor orientation for photogrammetric map compilation, *Photogramm. Eng. Remote Sens.* 75 (2009) 305–311.
- [9] C.V. Tao, Mobile mapping technology for road network data acquisition, *J. Geospatial Eng.* 2 (2000) 1–14.
- [10] J.F.C. Da Silva, P. de O. Camargo, R.B.A. Gallis, DEVELOPMENT OF A LOW-COST MOBILE MAPPING SYSTEM: A SOUTH AMERICAN EXPERIENCE, *Photogramm. Rec.* 18 (2003) 5–26. doi:10.1111/0031-868X.t01-1-00004.
- [11] D. Barber, J. Mills, S. Smith-Voysey, Geometric validation of a ground-based mobile laser scanning system, *ISPRS J. Photogramm. Remote Sens.* 63 (2008) 128–141. doi:10.1016/j.isprsjprs.2007.07.005.
- [12] I. Puente, H. González-Jorge, J. Martínez-Sánchez, P. Arias, Review of mobile mapping and surveying technologies, *Measurement*. 46 (2013) 2127–2145. doi:10.1016/j.measurement.2013.03.006.
- [13] K.P. Schwarz, N. El-Sheimy, Mobile Mapping Systems—State of the art and future trends, *Int. Arch. Photogramm. Remote Sens. Spat. Inf. Sci.* 35 (2004) 10 p.–10 p.
- [14] M.K. Kirchhöfer, J.H. Chandler, R. Wackrow, Testing and application of a low-cost photogrammetric recording system suitable for cultural heritage recording, in: *Vis. World From Sea-Bed to Cloud-Tops*, Remote Sensing and Photogrammetry Society, University College Cork and the National Maritime College of Ireland, 2010: p. 8.
- [15] M. Kirchhöfer, J. Chandler, R. Wackrow, Cultural heritage recording utilising low-cost close-range photogrammetry, in: *Proc. CIPA 23rd Int. Symp.*, Prague, Czech Republic, 2011: p. 8 p.
- [16] D. Hernández-López, M. Cabrelles, B. Felipe-García, J.L. Lerma, Calibration and Direct Georeferencing Analysis of a Multi-Sensor System for Cultural Heritage Recording, *Photogramm. - Fernerkundung - Geoinf.* 2012 (2012) 237–250. doi:10.1127/1432-8364/2012/0114.
- [17] J. Kim, S. Lee, H. Ahn, D. Seo, D. Seo, J. Lee, et al., Accuracy evaluation of a smartphone-based technology for coastal monitoring, *Meas. J. Int. Meas. Confed.* 46 (2013) 233–248. doi:10.1016/j.measurement.2012.06.010.
- [18] C.E.D.A. Freire, M. Painho, Development of a Mobile Mapping Solution for Spatial Data Collection Using Open-Source Technologies, *Procedia Technol.* 16 (2014) 481–490. doi:10.1016/j.protcy.2014.10.115.
- [19] J. Kelly, L.H. Matthies, G. Sukhatme, Simultaneous mapping and stereo extrinsic parameter calibration using GPS measurements, in: *Robot. Autom. (ICRA)*, 2011 IEEE Int. Conf., 2011: pp. 279–286. doi:10.1109/ICRA.2011.5980443.
- [20] N. Haala, J. Böhm, A multi-sensor system for positioning in urban environments, *ISPRS J. Photogramm. Remote Sens.* 58 (2003) 31–42. doi:10.1016/S0924-2716(03)00015-7.

- [21] D. Schleicher, L.M. Bergasa, M. Ocaña, R. Barea, M.E. López, Real-time hierarchical outdoor SLAM based on stereovision and GPS fusion, *Intell. Transp. Syst. IEEE Trans.* 10 (2009) 440–452.
- [22] T. Luhmann, Close range photogrammetry for industrial applications, *ISPRS Centen. Celebr. Issue.* 65 (2010) 558–569. doi:10.1016/j.isprsjprs.2010.06.003.
- [23] P. Patias, Medical imaging challenges photogrammetry, *ISPRS J. Photogramm. Remote Sens.* 56 (2002) 295–310. doi:10.1016/S0924-2716(02)00066-7.
- [24] K. Kraus, J. Jansa, H. Kager, *Photogrammetry, Vol. 2: Advanced methods and applications*, Dümmler, Bonn, 1997.
- [25] S. Cornou, M. Dhome, P. Sayd, Architectural reconstruction with multiple views and geometric constraints, in: *Br. Mach. Vis. Conf., The British Machine Vision Association and Society for Pattern Recognition*, Norwich, 2003; p. 10 p.
- [26] E. Grossmann, J. Santos-Victor, Least-squares 3D reconstruction from one or more views and geometric clues, *Comput. Vis. Image Underst.* 99 (2005) 151–174. doi:http://dx.doi.org/10.1016/j.cviu.2005.01.002.
- [27] J.D. Cothren, *Reliability in constrained Gauss-Markov models: an analytical and differential approach with applications in photogrammetry*, The Ohio State University, Columbus, Ohio, 2005.
- [28] J.C.K. Chow, D.D. Lichti, Photogrammetric Bundle Adjustment With Self-Calibration of the PrimeSense 3D Camera Technology: Microsoft Kinect, *Access, IEEE.* 1 (2013) 465–474. doi:10.1109/ACCESS.2013.2271860.
- [29] B.A. King, Bundle adjustment of constrained stereopairs- mathematical models, *Geomatics Res. Australas.* 63 (1995) 67–92.
- [30] N. Börlin, P. Grussenmeyer, J. Eriksson, P. Lindström, Pros and cons of constrained and unconstrained formulation of the bundle adjustment problem, *Int. Arch. Photogramm. Remote Sensing, Spat. Inf. Sci.* 35 (2004) 589–594.
- [31] Y.-J. Lee, A. Yilmaz, Temporal geometric constrained bundle adjustment for the aerial multi-head camera system, in: *Orlando, Florida, 2010*.
- [32] J.L. Lerma, S. Navarro, M. Cabrelles, A.E. Seguí, Camera Calibration with Baseline Distance Constraints, *Photogramm. Rec.* 25 (2010) 140–158. doi:10.1111/j.1477-9730.2010.00579.x.
- [33] A. Habib, A.P. Kersting, K. Bang, J. Rau, A Novel Single-step Procedure for the Calibration of the Mounting Parameters of a multi-camera Terrestrial Mobile Mapping System, in: *Proceeding 7th Int. Symp. Mob. Mapp. Technol. Pol.*, 2011; pp. 173–185.
- [34] A.M.G. Tommaselli, M.V.A. Moraes, J. Marcato Junior, C.R.T. Caldeira, R.F. Lopes, M. Galo, Using Relative Orientation Constraints to Produce Virtual Images from Oblique Frames, *Proc. XXII ISPRS Congr. Melbourne, Aust.* 39 (2012) 61–66.
- [35] M.I. Alba, L. Barazzetti, M. Scaioni, E. Rosina, M. Previtali, Mapping Infrared Data on Terrestrial Laser Scanning 3D Models of Buildings, *Remote Sens.* 3 (2011) 1847–1870. doi:10.3390/rs3091847.

- [36] A.H. Ahmadabadian, S. Robson, J. Boehm, M. Shortis, K. Wenzel, D. Fritsch, A comparison of dense matching algorithms for scaled surface reconstruction using stereo camera rigs, *ISPRS J. Photogramm. Remote Sens.* 78 (2013) 157–167. doi:10.1016/j.isprsjprs.2013.01.015.
- [37] Y.-J. Lee, A. Yilmaz, Bore-sight calibration of the aerial multi-head camera system, in: M. Blowers, T.H. O'Donnell, O.L. Mendoza-Schrock (Eds.), *Evol. Bio-Inspired Comput. Theory Appl. V*, Orlando, Florida, USA, 2011: pp. 805906–805908. doi:10.1117/12.888871.
- [38] A.M.G. Tommaselli, M. Galo, W.S. Bazan, R.S. Ruy, J.M. Junior, Simultaneous calibration of multiple camera heads with fixed base constraint, in: São Paulo, Brazil, 2009.
- [39] A.M.G. Tommaselli, M. Galo, M.V.A. de Moraes, J. Marcato, C.R.T. Caldeira, R.F. Lopes, Generating Virtual Images from Oblique Frames, *Remote Sens.* 5 (2013) 1875–1893.
- [40] A. Gruen, H. Beyer, System Calibration Through Self-Calibration, in: A. Gruen, T. Huang (Eds.), *Calibration Orientat. Cameras Comput. Vis. SE - 7*, Springer Berlin Heidelberg, 2001: pp. 163–193. doi:10.1007/978-3-662-04567-1_7.
- [41] J.L. Lerma, S. Navarro, M. Cabrelles, A.E. Seguí, D. Hernández-López, Automatic orientation and 3D modelling from markerless rock art imagery, *ISPRS J. Photogramm. Remote Sens.* 76 (2013) 64–75. doi:10.1016/j.isprsjprs.2012.08.002.
- [42] B. Ruzgienė, T. Berteška, S. Gečyte, E. Jakubauskienė, V.Č. Aksamitauskas, The surface modelling based on UAV Photogrammetry and qualitative estimation, *Measurement.* 73 (2015) 619–627. doi:10.1016/j.measurement.2015.04.018.